Enhancement of thrust performance of a MPD thruster with a magnetic nozzle

IEPC-2013-338

Presented at the 33rd International Electric Propulsion Conference,
The George Washington University • Washington, D.C. • USA
October 6 – 10, 2013

Akira Ando, Kazunori Takahashi, Yuuki Izawa, Kiyotaka Suzuki, Yusuke Hoshino
Department of Electrical Engineering, Tohoku University, Sendai, 980-8579, Japan

Abstract: An applied field Magneto-Plasma-Dynamic thruster was investigated using a pendulum type thrust target. Thrust, specific impulse and thrust efficiency were measured by the target and thrust of more than 7N was attained in hydrogen propellant by applying a diverging magnetic nozzle. Axial flow velocity of the exhausted helium plasma attained to 40 km/sec near the thruster exit and aximuthal plasma rotation was observed caused by JxB force. Sudden increase of an ion temperature was appeared in the downstream region, whereas the plasma flow decelerated simultaneously.

Nomenclature

I_d	=	discharge current			
Z	=	axial position	Y	=	radial position
B_0	=	uniform magnetic field strength			
B_{ZC}	=	peak magnetic field strength of external magnetic coil			
F	=	thrust			
I_{sp}	=	specific impulse			
U_z	=	axial flow velocity	U_θ	=	axial flow velocity
T_i	=	ion temperature			

I. Introduction

AN electric propulsion system is one of the key elements in future space exploration projects and has been developed for various space missions. [1),2)] Development of a high power-density plasma thruster with a higher specific impulse and a larger thrust is prerequisite for a manned interplanetary space thruster. A Magneto-Plasma-Dynamic (MPD) thruster has been developed as one of a high enthalpy plasma source with a high-specific impulse for space mission targeting from orbital maneuver to interplanetary transportation. It is also expected as one of the promising candidates for a manned interplanetary space thruster with higher specific impulse and larger thrust. In order to improve thrust performance of a MPD thruster, it has been proposed to operate it with various types of an externally applied axial magnetic field. Researches on a MPD thruster with an applied magnetic field have been performed in order to enhance its efficiency and to reduce heat loss in its electrodes. [3)-6)]

So far, we have investigated an applied field MPD thruster, where an axial diverging magnetic nozzle was formed near the exit of the thruster. The plasma flow field and electromagnetic field were measured near the exit. The plasma was accelerated by the electromagnetic force and a Mach number of the flow increased by aerodynamic effect, resulting in generation of a supersonic plasma flow in the diverging magnetic nozzle.[7)-9)] Further, utilizing a magnetic nozzle downstream, we have successfully realized a supersonic and super-Alfvénic plasma flow. It is important not only to clarify the mechanism of the applied field MPD operation, but to verify the plasma detachment from the magnetic field. [10)]

In order to evaluate thrust performance of an applied field MPD thruster, we measured a thrust using a pendulum type thrust target and the effect of the shape and strength of the external magnetic field are experimentally investigated.

II. Experimental setup

A. The HITOP device and an MPD thruster

Experiments were carried out in the HITOP device of Tohoku University. It consists of a large cylindrical vacuum chamber (diameter D = 0.8m, length L = 3.3m) with eleven main and six auxiliary magnetic coils, which generate a uniform magnetic field up to 0.1T. Various types of magnetic field configuration can be formed by adjusting an external coil current. A high power MPD thruster was installed at one end-port of the HITOP. It has a coaxial structure with a center tungsten rod cathode (10mm in diameter) and an annular molybdenum anode (30mm in diameter). A discharge current I_d up to 10kA is supplied by a pulse-forming network (PFN) system with the quasi-steady duration of 1ms. The current I_d is kept nearly constant during a discharge with a typical voltage of 200V-300V and can be controlled by varying a charging voltage of capacitor banks of the PFN power-supply. It can generate a high density (more than $10^{20}m^{-3}$) plasma.

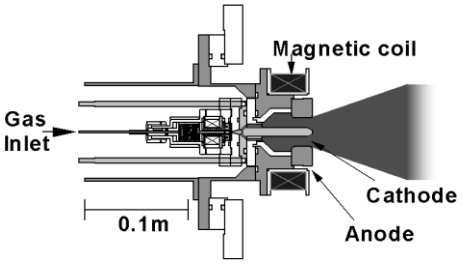

Figure 1. Schematic of a MPD thruster with an external magnetic coil.

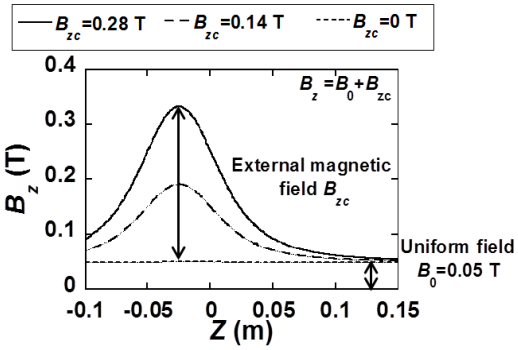

Figure 2. S Spatial profiles of the pulsed magnetic fields by the magnetic coil attached on the MPDT.

Schematic of the MPD thruster is shown in Fig.1. An external magnetic coil is attached on the MPD, which can generate an axial magnetic field up to 0.8T with the pulse duration of 10ms. Spatial profiles by the magnetic coil are shown in Fig.2. The field strength generated by the external coil is defined as the magnetic nozzle intensity B_{zc} shown in Fig.2. Here, the position of Z=0 corresponds to the tip position of the cathode. With the applied magnetic field, a diverging magnetic nozzle is formed at the muzzle of the MPD thruster. In this experiment a uniform magnetic field B_0 was also applied with the pulsed magnetic nozzle field. It prevents plasma scattering for thrust measurement using a thrust target. It does not contribute to the plasma acceleration in the axial direction. Three configurations shown in Fig.2 were tested with B_{zc} =0 T, 0.14 T and 0.28 T, respectively, and the uniform field B_0=0.05 T.

B. Thrust target

In order to measure the thrust generated in the applied field MPDT, a pendulum type thrust target was installed inside the HITOP vacuum chamber as shown in Fig. 3. The thrust target has a cylindrical structure consisting of 14 ring plates with center holes (16-cm-diameter) and a bottom cone plate made of stainless steel. Plasma plume enters the cylindrical target through the center hole and collides with the bottom cone plate and reflects as neutral particles by recombination on the plate. The particle reflection results in overestimate of the thrust. However, most of reflected particles from the bottom plate escape radially from the side slits, so axial momentum is converted into radial momentum. This structure minimizes the particle reflection effects on the thrust measurement.[11),12)]

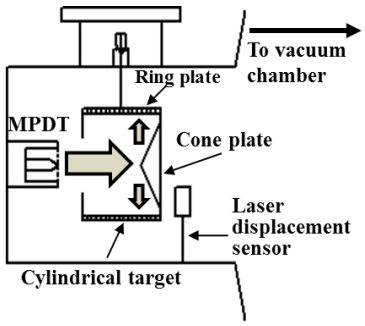

Figure 3. Schematic of a pendulum type thrust target located in front of a MPD thruster.

The impulse bit ($I_{bit} = F\ \Delta t$) was estimated from an swing amplitude of the target, which was measured by a laser displacement sensor. The calibration coefficient between the swing amplitude and the impulse bit was obtained before pumping down the chamber and was confirmed to be unchanged after evacuating the chamber. The discharge pulse width Δt was around 1ms, which was evaluated from a waveform of discharge current. The specific impulse is also

calculated with the given mass flow rate of the propellant gas.

C. Spectroscopy

The exhausted plasma flow velocity and ion temperature were measured in He plasma by an Optical Emission Spectroscopy (OES). An optical lens and a fiber are mounted on a movable optical stages and light emitted from the plasma was monitored by a spectrometer through the optical fiber. The evaluation of Doppler shift gives a plasma flow velocity U_z, ion temperature T_i and plasma rotating velocity U_θ, where He II line (λ_0=468.575 nm) was used as a measured spectrum. [13)-14)]

III. Experimental results

A. Thrust measurement

We have investigated thrust performance in an applied field MPD thruster shown in Fig.1 in order to investigate the effect of applied field on a MPD thruster. Different propellant gases, Ar, He and H_2 were tested with the diverging magnetic field applied to the MPD thruster. Thrust and specific impulse were measured using the pendulum type thrust target.

Figure 4 shows thrust and specific impulse with Ar propellant. They increased with a discharge current I_d and applied magnetic field intensity. We have also changed the coil position near the muzzle of the MPDT. Maximum thrust was obtained when the peak position of the applied magnetic field was set upstream of the muzzle of MPDT, which corresponds to the profile of Fig.2.

Thrust efficiency was calculated including consumed power in the magnetic coil. Although it was around several % in Ar propellant and nearly constant with I_d, it increased with the applied magnetic field.

Figure 5 and 6 shows thrust and specific impulse with He and H_2, respectively. They also increased with a discharge current and applied magnetic field intensity. Thrust attained more than 7 N in hydrogen gas with I_d = 6 kA and B_{zc} = 0.28 T. The thrust almost doubles with respect to no diverging magnetic field B_{zc}.

The thrust efficiency also increased in He and H_2 with applied magnetic field. It increased with discharge current unlike in the case of Ar and attained 20% in He and nearly 50% in H_2.

In order to clarify the improvement of the applied field MPD thruster, thrust was also estimated from the exhausted plasma flow parameters. Plasma density and temperature were measured by Langmuir probe and flow velocity was estimated by spectroscopy and a time-of-flight method of ion saturation currents. The plasma flow velocity increased with discharge current. Although it was saturated close to the Alfvén critical velocity, it increased more than the critical velocity with increase of the applied magnetic

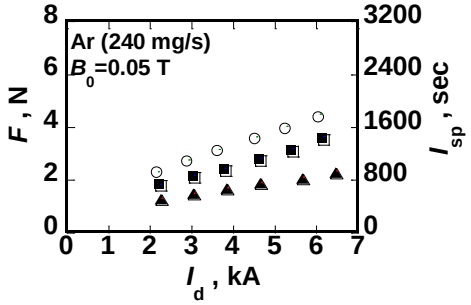

Figure 4. Thrust F and specific impulse I_{sp} as a function of discharge current I_d. Ar gas with mass flow rate of dm/dt=0.24g/s. Open circles: B_{zc} = 0.28 T, closed squares: B_{zc} = 0.14 T and closed triangles: B_{zc} = 0 T.

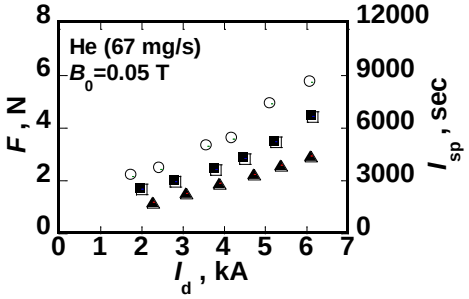

Figure 5. Thrust F and specific impulse I_{sp} as a function of discharge current I_d. He gas with mass flow rate of dm/dt=0.067g/s. Symbols are the same as in Fig.4.

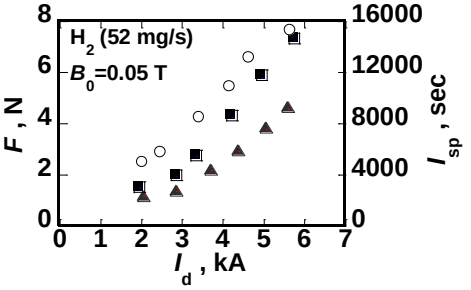

Figure 6. Thrust F and specific impulse I_{sp} as a function of discharge current I_d. H_2 gas with mass flow rate of dm/dt=0.052g/s. Symbols are the same as in Fig.4.

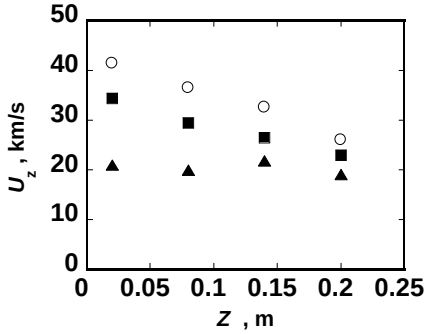

Figure 7. Axial profile of plasma flow velocity. I_d=7.1kA. He gas with mass flow rate of dm/dt=0.067g/s. Symbols are the same as in Fig.4.

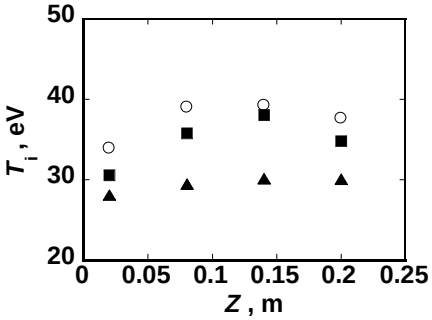

Figure 8. Axial profile of ion temperature. Conditions were the same as in Fig.7.

field.

B. Plasma parameters measurement by OES

The plume plasma velocity and ion temperature were measured by spectroscopy in He propellant. Figure 7 and 8 shows the axial profiles of plasma flow velocity U_z and ion temperature T_i with the three magnetic field, respectively. As the HeII optical emission was significantly weak for the current less than 6 kA, the OES measurement was performed at 7.1 kA. The results show that U_z and T_i increased with increasing B_{zc} near the muzzle of the MPDT.

U_z attains to 40km/s at Z = 2 cm, and decreased gradually in the downstream region, where ion temperature increased. The ion Mach number was calculated in the exhausting plasma and was slightly below unity at Z = 2 cm.

These data suggests that the axial plasma flow energy is converted to the thermal energy in the diverging magnetic field according to the isentropic flow model passing through varying cross section. When the nozzle cross sectional area gradually increased, flow velocity decreases and temperature of passing fluid increases. In the applied-field MPD thruster, electrons are magnetized and flow along the field lines. Although ions are unmagnetized, they also limited by the field line by electric force between electrons and ions. Ions behave as ion fluids passing through a tube. The increase of the ion temperature indicates that the flow energy was converted into the thermal energy in the divergent magnetic nozzle field.

Figure 9 shows a spatial profile of emission intensity of He II line. In the downstream region the intensity abruptly increased, which indicates rapid increase of plasma density.

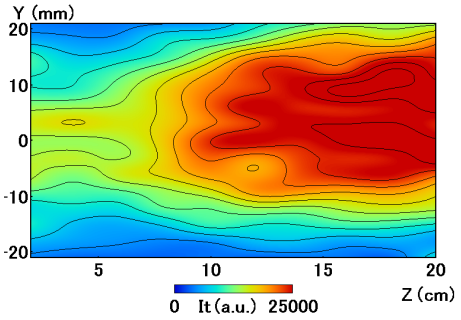

Figure 9. Spatial profile of line emission intensity of HeII. Conditions were the same as in Fig.7.

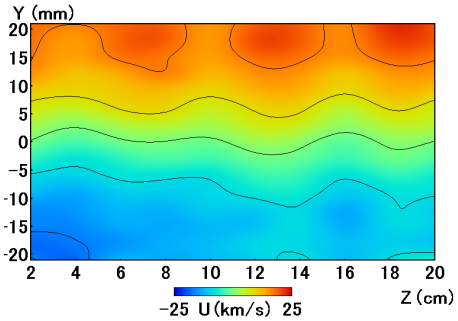

Figure 10. Spatial profile of azimuthal rotation velocity U_θ. Conditions were the same as in Fig.7.

Figure 10 shows a spatial profile of azimuthal flow velocity. The radial profile of the rotation velocity shows the plasma rotates as a rigid body in the center region. The rotation direction corresponds to that of JxB force.

These measurements of plasma plume indicate that flow energy was converted into the thermal energy at the end of magnetic nozzle in the exhausted plasma. Further improvement of thrust performance is expected by avoiding the energy transfer using a Laval-type magnetic nozzle. Further experiments will be performed in near future.

IV. Conclusion

In order to investigate effects of the applied magnetic nozzle on a Magneto-Plasma-Dynamic thruster, thrust was measured using a pendulum type thrust target in Ar, He and H_2 as propellant gas. It increased with discharge current and applied diverging magnetic nozzle field and attained more than 7N was attained in hydrogen propellant. Thrust efficiency considering consumed power in the external coils was also calculated. It increased by applying the magnetic field and the efficiency of nearly 50% was obtained in hydrogen propellant. Axial flow velocity of the exhausted helium plasma were measured by spectroscopy and it attained to 40 km/sec near the thruster exit. Azimuthal plasma rotation caused by JxB force was also observed. Sudden increase of an ion temperature was appeared in the downstream region, whereas the plasma flow decelerated simultaneously, which indicates that the flow energy is converted into the thermal energy in the divergent magnetic nozzle field according to the isentropic flow model.

Acknowledgments

The authors would like to thank H. Ishida for his technical assistance.

References

[1] Frisbee. R.H., "Advanced Space Propulsion for the 21st Century," *J. Propulsion and Power*, Vol.19, No.6, 2003, pp.1129-1154.

[2] Sankaran K., Cassady L., Kodys A. D. and Choueiri E.Y., "A survey of propulsion options for cargo and piloted missions to Mars", Ann. N. Y. Acad. Sci., Vol.1017, No.1, 2004, 450-467.

[3] Tahara H., Takiguchi F., Kagaya Y. and Yoshikawa T., "Performance characteristics and discharge features of aquasi-steady applied-field MPD arcjet" IEPC-91-073, 22nd Int. Electric Propulsion Conference, 1991.

[4] Sasoh A., "Generalized Hall Acceleration", Journal of Propulsion and Power, Vol.10 (1994) 251-254.

[5] Coletti M., "A thrust formula for an MPD thruster with applied-magnetic field" Acta Astronautica Vol. 81 (2012) 667-674.

[6] Hoyt R. P., "Magnetic nozzle design for high-power MPD thrusters" IEPC-2005-230, 29th International Electric Propulsion Conference, 2005.

[7] Inutake, M., Ando, A., et al., "Improvement of an MPD Thruster Performance with a Laval-type Magnetic Nozzle," Proceedings of the 29th International Electric Propulsion Conference, IEPC-2005-83, 2005.

[8] Inutake M., Ando A., Hattori K., Tobari H. Makita T., Isobe H., and Komagome T., "Transonic plasma flow passing through a magnetic mirror," Transactions of Fusion Technology, Vol.51, No.2T, FUSTE8, 2007, pp.141-146.

[9] Inutake M., Ando A., Hattori K., Tobari H. Makita T., Shibata M., Y. Kasashima, and Komagome T., "Generation of supersonic plasma flows using an applied-field MPD arcjet and ICRF heating," Plasma Physics and Controlled Fusion, Vol.49, 2007, pp.A121-A134.

[10] Ando A., et al., "Generation of Supersonic and Super-Alfvenic Flow Using ICRF Heating and a Magnetic Nozzle", Plasma and Fusion Research, Vol.3, 2008, pp.S1018_1-4.

[11] Yanagi R., Kimura I., "New Type of Target for the Measurement of Impulse Bits of Pulsed Plasma Thrusters", Journal of Spacecraft and Rockets, Vol.19, 1982, pp.246-249.

[12] Coletti, M. Balestra A., Sensini M. and Paccani G., "Solid State MPD Thruster with Applied Magnetic Field", IEPC-2007-158, 30th International Electric Propulsion Conference, 2007.

[13] Ando A., Ashino M., Sagi Y., Inutake M., and Hattori K. i, M.Yoshinuma, A.Imasaki, H. Tobari and T.Yagai, "Spectroscopic Studies of a High Mach-Number Rotating Plasma Flow", J. Plasma Fusion Res. SERIES Vol.4, 2001, pp. 373-378.

[14] Tobari H., Ando A., Inutake M., Hattori K., "Characteristics of electromagnetically accelerated plasma flow in an externally-applied magnetic field," Physics of Plasmas, Vol.14, 2007, pp.093507_1-10.